

Constraints on the origin of cosmic rays above 10^{18} eV from large scale anisotropy searches in data of the Pierre Auger Observatory

The Pierre Auger Collaboration[†]

- P. Abreu⁶³, M. Aglietta⁵¹, M. Ahlers⁹⁴, E.J. Ahn⁸¹, I.F.M. Albuquerque¹⁵, D. Allard²⁹, I. Allekotte¹, J. Allen⁸⁵, P. Allison⁸⁷, A. Almela^{11, 7}, J. Alvarez Castillo⁵⁶, J. Alvarez-Muñiz⁷³, R. Alves Batista¹⁶, M. Ambrosio⁴⁵, A. Aminaei⁵⁷, L. Anchordoqui⁹⁵, S. Andringa⁶³, T. Antičić²³, C. Aramo⁴⁵, E. Arganda^{4, 70}, F. Arqueros⁷⁰, H. Asorey¹, P. Assis⁶³, J. Aublin³¹, M. Ave³⁷, M. Avenier³², G. Avila¹⁰, A.M. Badescu⁶⁶, M. Balzer³⁶, K.B. Barber¹², A.F. Barbosa^{13 ‡}, R. Bardenet³⁰, S.L.C. Barroso¹⁸, B. Baughman^{87 f}, J. Bäuml³⁵, C. Baus³⁷, J.J. Beatty⁸⁷, K.H. Becker³⁴, A. Bellétoile³³, J.A. Bellido¹², S. BenZvi⁹⁴, C. Berat³², X. Bertou¹, P.L. Biermann³⁸, P. Billoir³¹, F. Blanco⁷⁰, M. Blanco^{31, 71}, C. Bleve³⁴, H. Blümer^{37, 35}, M. Boháčová²⁵, D. Boncioli⁴⁶, C. Bonifazi^{21, 31}, R. Bonino⁵¹, N. Borodai⁶¹, J. Brack⁷⁹, I. Brancus⁶⁴, P. Brogueira⁶³, W.C. Brown⁸⁰, R. Bruijn^{75 i}, P. Buchholz⁴¹, A. Bueno⁷², L. Buroker⁹⁵, R.E. Burton⁷⁷, K.S. Caballero-Mora⁸⁸, B. Caccianiga⁴⁴, L. Caramete³⁸, R. Caruso⁴⁷, A. Castellina⁵¹, O. Catalano⁵⁰, G. Cataldi⁴⁹, L. Cazon⁶³, R. Cester⁴⁸, J. Chauvin³², S.H. Cheng⁸⁸, A. Chiavassa⁵¹, J.A. Chinellato¹⁶, J. Chirinos Diaz⁸⁴, J. Chudoba²⁵, M. Cilmo⁴⁵, R.W. Clay¹², G. Cocciolo⁴⁹, L. Collica⁴⁴, M.R. Coluccia⁴⁹, R. Conceição⁶³, F. Contreras⁹, H. Cook⁷⁵, M.J. Cooper¹², J. Coppens^{57, 59}, A. Cordier³⁰, S. Couturier⁸⁸, C.E. Covault⁷⁷, A. Creusot²⁹, A. Criss⁸⁸, J. Cronin⁹⁰, A. Curutiu³⁸, S. Dagoret-Campagne³⁰, R. Dallier³³, B. Daniel¹⁶, S. Dasso^{5, 3}, K. Daumiller³⁵, B.R. Dawson¹², R.M. de Almeida²², M. De Domenico⁴⁷, C. De Donato⁵⁶, S.J. de Jong^{57, 59}, G. De La Vega⁸, W.J.M. de Mello Junior¹⁶, J.R.T. de Mello Neto²¹, I. De Mitri⁴⁹, V. de Souza¹⁴, K.D. de Vries⁵⁸, L. del Peral⁷¹, M. del Río^{46, 9}, O. Deligny²⁸, H. Dembinski³⁷, N. Dhital⁸⁴, C. Di Giulio^{46, 43}, M.L. Díaz Castro¹³, P.N. Diep⁹⁶, F. Diogo⁶³, C. Dobrigkeit¹⁶, W. Docters⁵⁸, J.C. D'Olivo⁵⁶, P.N. Dong^{96, 28}, A. Dorofeev⁷⁹, J.C. dos Anjos¹³, M.T. Dova⁴, D. D'Urso⁴⁵, I. Dutan³⁸, J. Ebr²⁵, R. Engel³⁵, M. Erdmann³⁹, C.O. Escobar^{81, 16}, J. Espadanal⁶³, A. Etchegoyen^{7, 11}, P. Facial San Luis⁹⁰, H. Falcke^{57, 60, 59}, K. Fang⁹⁰, G. Farrar⁸⁵, A.C. Fauth¹⁶, N. Fazzini⁸¹, A.P. Ferguson⁷⁷, B. Fick⁸⁴, J.M. Figueira⁷, A. Filevich⁷, A. Filipčič^{67, 68}, S. Fliescher³⁹, C.E. Fracchiolla⁷⁹, E.D. Fraenkel⁵⁸, O. Fratu⁶⁶, U. Fröhlich⁴¹, B. Fuchs³⁷, R. Gaior³¹, R.F. Gamarra⁷, S. Gambetta⁴², B. García⁸, S.T. Garcia Roca⁷³, D. Garcia-Gamez³⁰, D. Garcia-Pinto⁷⁰, G. Garilli⁴⁷, A. Gascon Bravo⁷², H. Gemmeke³⁶, P.L. Ghia³¹, M. Giller⁶², J. Gitto⁸, H. Glass⁸¹, M.S. Gold⁹³, G. Golup¹, F. Gomez Albarracin⁴, M. Gómez Berisso¹, P.F. Gómez Vitale¹⁰, P. Gonçalves⁶³, J.G. Gonzalez³⁵, B. Gookin⁷⁹, A. Gorgi⁵¹, P. Gouffon¹⁵, E. Grashorn⁸⁷, S. Grebe^{57, 59}, N. Griffith⁸⁷, A.F. Grillo⁵², Y. Guardincerri³, F. Guarino⁴⁵, G.P. Guedes¹⁷, P. Hansen⁴, D. Harari¹, T.A. Harrison¹², J.L. Harton⁷⁹, A. Haungs³⁵, T. Hebbeker³⁹, D. Heck³⁵, A.E. Herve¹², G.C. Hill¹², C. Hojvat⁸¹, N. Hollon⁹⁰, V.C. Holmes¹², P. Homola⁶¹, J.R. Hörandel^{57, 59}, P. Horvath²⁶, M. Hrabovsky^{26, 25}, D. Huber³⁷, T. Huege³⁵, A. Insolia⁴⁷, F. Ionita⁹⁰, A. Italiano⁴⁷, S. Jansen^{57, 59}, C. Jarne⁴, S. Jiraskova⁵⁷, M. Josebachuili⁷, K. Kadija²³, K.H. Kampert³⁴, P. Karhan²⁴, P. Kasper⁸¹, I. Katkov³⁷, B. Kégl³⁰, B. Keilhauer³⁵, A. Keivani⁸³, J.L. Kelley⁵⁷, E. Kemp¹⁶, R.M. Kieckhafer⁸⁴, H.O. Klages³⁵, M. Kleifges³⁶, J. Kleinfellner^{9, 35}, J. Knapp⁷⁵, D.-H. Koang³²,

K. Kotera⁹⁰, N. Krohm³⁴, O. Krömer³⁶, D. Kruppke-Hansen³⁴, D. Kuempel^{39, 41}, J.K. Kulbartz⁴⁰, N. Kunka³⁶, G. La Rosa⁵⁰, C. Lachaud²⁹, D. LaHurd⁷⁷, L. Latronico⁵¹, R. Lauer⁹³, P. Lautridou³³, S. Le Coz³², M.S.A.B. Leão²⁰, D. Lebrun³², P. Lebrun⁸¹, M.A. Leigui de Oliveira²⁰, A. Letessier-Selvon³¹, I. Lhenry-Yvon²⁸, K. Link³⁷, R. López⁵³, A. Lopez Agüera⁷³, K. Louedec^{32, 30}, J. Lozano Bahilo⁷², L. Lu⁷⁵, A. Lucero⁷, M. Ludwig³⁷, H. Lyberis^{21, 28}, M.C. Maccarone⁵⁰, C. Macolino³¹, S. Maldera⁵¹, J. Maller³³, D. Mandat²⁵, P. Mantsch⁸¹, A.G. Mariazzi⁴, J. Marin^{9, 51}, V. Marin³³, I.C. Maris³¹, H.R. Marquez Falcon⁵⁵, G. Marsella⁴⁹, D. Martello⁴⁹, L. Martin³³, H. Martinez⁵⁴, O. Martínez Bravo⁵³, D. Martraire²⁸, J.J. Masías Meza³, H.J. Mathes³⁵, J. Matthews⁸³, J.A.J. Matthews⁹³, G. Matthiae⁴⁶, D. Maurel³⁵, D. Maurizio^{13, 48}, P.O. Mazur⁸¹, G. Medina-Tanco⁵⁶, M. Melissas³⁷, D. Melo⁷, E. Menichetti⁴⁸, A. Menshikov³⁶, P. Mertsch⁷⁴, S. Messina⁵⁸, C. Meurer³⁹, R. Meyhandan⁹¹, S. Mi'canović²³, M.I. Micheletti⁶, I.A. Minaya⁷⁰, L. Miramonti⁴⁴, L. Molina-Bueno⁷², S. Mollerach¹, M. Monasor⁹⁰, D. Monnier Ragaigne³⁰, F. Montanet³², B. Morales⁵⁶, C. Morello⁵¹, E. Moreno⁵³, J.C. Moreno⁴, M. Mostafá⁷⁹, C.A. Moura²⁰, M.A. Muller¹⁶, G. Müller³⁹, M. Münchmeyer³¹, R. Mussa⁴⁸, G. Navarra⁵¹ ‡, J.L. Navarro⁷², S. Navas⁷², P. Necesal²⁵, L. Nellen⁵⁶, A. Nelles^{57, 59}, J. Neuser³⁴, P.T. Nhung⁹⁶, M. Niechciol⁴¹, L. Niemietz³⁴, N. Nierstenhoefer³⁴, D. Nitz⁸⁴, D. Nosek²⁴, L. Nožka²⁵, J. Oehlschläger³⁵, A. Olinto⁹⁰, M. Ortiz⁷⁰, N. Pacheco⁷¹, D. Pakk Selmi-Dei¹⁶, M. Palatka²⁵, J. Pallotta², N. Palmieri³⁷, G. Parente⁷³, E. Parizot²⁹, A. Parra⁷³, S. Pastor⁶⁹, T. Paul⁸⁶, M. Pech²⁵, J. Pękala⁶¹, R. Pelayo^{53, 73}, I.M. Pepe¹⁹, L. Perrone⁴⁹, R. Pesce⁴², E. Petermann⁹², S. Petrera⁴³, A. Petrolini⁴², Y. Petrov⁷⁹, C. Pfendner⁹⁴, R. Piegaia³, T. Pierog³⁵, P. Pieroni³, M. Pimenta⁶³, V. Pirronello⁴⁷, M. Platino⁷, M. Plum³⁹, V.H. Ponce¹, M. Pontz⁴¹, A. Porcelli³⁵, P. Privitera⁹⁰, M. Prouza²⁵, E.J. Quel², S. Querchfeld³⁴, J. Rautenberg³⁴, O. Ravel³³, D. Ravignani⁷, B. Revenu³³, J. Ridky²⁵, S. Riggi⁷³, M. Risso⁴¹, P. Ristori², H. Rivera⁴⁴, V. Rizi⁴³, J. Roberts⁸⁵, W. Rodrigues de Carvalho⁷³, G. Rodriguez⁷³, I. Rodriguez Cabo⁷³, J. Rodriguez Martino⁹, J. Rodriguez Rojo⁹, M.D. Rodríguez-Frías⁷¹, G. Ros⁷¹, J. Rosado⁷⁰, T. Rossler²⁶, M. Roth³⁵, B. Rouillé-d'Orfeuil⁹⁰, E. Roulet¹, A.C. Rovero⁵, C. Rühle³⁶, A. Saftoiu⁶⁴, F. Salamida²⁸, H. Salazar⁵³, F. Salesa Greus⁷⁹, G. Salina⁴⁶, F. Sánchez⁷, C.E. Santo⁶³, E. Santos⁶³, E.M. Santos²¹, F. Sarazin⁷⁸, B. Sarkar³⁴, S. Sarkar⁷⁴, R. Sato⁹, N. Scharf³⁹, V. Scherini⁴⁴, H. Schieler³⁵, P. Schiffer^{40, 39}, A. Schmidt³⁶, O. Scholten⁵⁸, H. Schoorlemmer^{57, 59}, J. Schovancova²⁵, P. Schovánek²⁵, F. Schröder³⁵, D. Schuster⁷⁸, S.J. Sciutto⁴, M. Scuderi⁴⁷, A. Segreto⁵⁰, M. Settimo⁴¹, A. Shadkam⁸³, R.C. Shellard¹³, I. Sidelnik⁷, G. Sigl⁴⁰, H.H. Silva Lopez⁵⁶, O. Sima⁶⁵, A. Smiałkowski⁶², R. Šmídá³⁵, G.R. Snow⁹², P. Sommers⁸⁸, J. Sorokin¹², H. Spinka^{76, 81}, R. Squartini⁹, Y.N. Srivastava⁸⁶, S. Stanic⁶⁸, J. Stapleton⁸⁷, J. Stasielak⁶¹, M. Stephan³⁹, A. Stutz³², F. Suarez⁷, T. Suomijärvi²⁸, A.D. Supanitsky⁵, T. Šuša²³, M.S. Sutherland⁸³, J. Swain⁸⁶, Z. Szadkowski⁶², M. Szuba³⁵, A. Tapia⁷, M. Tartare³², O. Taşcău³⁴, R. Tcaciu⁴¹, N.T. Thao⁹⁶, D. Thomas⁷⁹, J. Tiffenberg³, C. Timmermans^{59, 57}, W. Tkaczyk⁶² ‡, C.J. Todero Peixoto¹⁴, G. Toma⁶⁴, L. Tomankova²⁵, B. Tome⁶³, A. Tonachini⁴⁸, G. Torralba Elipe⁷³, P. Travnicek²⁵, D.B. Tridapalli¹⁵, G. Tristram²⁹, E. Trovato⁴⁷, M. Tueros⁷³, R. Ulrich³⁵, M. Unger³⁵, M. Urban³⁰, J.F. Valdés Galicia⁵⁶, I. Valiño⁷³, L. Valore⁴⁵, G. van Aar⁵⁷, A.M. van den Berg⁵⁸, S. van Velzen⁵⁷, A. van Vliet⁴⁰,

E. Varela⁵³, B. Vargas Cárdenas⁵⁶, J.R. Vázquez⁷⁰, R.A. Vázquez⁷³, D. Veberič^{68, 67}, V. Verzi⁴⁶, J. Vicha²⁵, M. Videla⁸, L. Villaseñor⁵⁵, H. Wahlberg⁴, P. Wahrlich¹², O. Wainberg^{7, 11}, D. Walz³⁹, A.A. Watson⁷⁵, M. Weber³⁶, K. Weidenhaupt³⁹, A. Weindl³⁵, F. Werner³⁵, S. Westerhoff⁹⁴, B.J. Whelan^{88, 12}, A. Widom⁸⁶, G. Wieczorek⁶², L. Wiencke⁷⁸, B. Wilczyńska⁶¹, H. Wilczyński⁶¹, M. Will³⁵, C. Williams⁹⁰, T. Winchen³⁹, M. Wommer³⁵, B. Wundheiler⁷, T. Yamamoto^{90 a}, T. Yapici⁸⁴, P. Younk^{41, 82}, G. Yuan⁸³, A. Yushkov⁷³, B. Zamorano Garcia⁷², E. Zas⁷³, D. Zavrtanik^{68, 67}, M. Zavrtanik^{67, 68}, I. Zaw^{85 h}, A. Zepeda^{54 b}, J. Zhou⁹⁰, Y. Zhu³⁶, M. Zimbres Silva^{34, 16}, M. Ziolkowski⁴¹

† *Av. San Martín Norte 306, 5613 Malargüe, Mendoza, Argentina; www.auger.org*

¹ *Centro Atómico Bariloche and Instituto Balseiro (CNEA-UNCuyo-CONICET), San Carlos de Bariloche, Argentina*

² *Centro de Investigaciones en Láseres y Aplicaciones, CITEDEF and CONICET, Argentina*

³ *Departamento de Física, FCEyN, Universidad de Buenos Aires y CONICET, Argentina*

⁴ *IFLP, Universidad Nacional de La Plata and CONICET, La Plata, Argentina*

⁵ *Instituto de Astronomía y Física del Espacio (CONICET-UBA), Buenos Aires, Argentina*

⁶ *Instituto de Física de Rosario (IFIR) - CONICET/U.N.R. and Facultad de Ciencias Bioquímicas y Farmacéuticas U.N.R., Rosario, Argentina*

⁷ *Instituto de Tecnologías en Detección y Astropartículas (CNEA, CONICET, UNSAM), Buenos Aires, Argentina*

⁸ *National Technological University, Faculty Mendoza (CONICET/CNEA), Mendoza, Argentina*
⁹ *Observatorio Pierre Auger, Malargüe, Argentina*

¹⁰ *Observatorio Pierre Auger and Comisión Nacional de Energía Atómica, Malargüe, Argentina*

¹¹ *Universidad Tecnológica Nacional - Facultad Regional Buenos Aires, Buenos Aires, Argentina*
¹² *University of Adelaide, Adelaide, S.A., Australia*

¹³ *Centro Brasileiro de Pesquisas Fisicas, Rio de Janeiro, RJ, Brazil*

¹⁴ *Universidade de São Paulo, Instituto de Física, São Carlos, SP, Brazil*

¹⁵ *Universidade de São Paulo, Instituto de Física, São Paulo, SP, Brazil*

¹⁶ *Universidade Estadual de Campinas, IFGW, Campinas, SP, Brazil*

¹⁷ *Universidade Estadual de Feira de Santana, Brazil*

¹⁸ *Universidade Estadual do Sudoeste da Bahia, Vitoria da Conquista, BA, Brazil*

¹⁹ *Universidade Federal da Bahia, Salvador, BA, Brazil*

²⁰ *Universidade Federal do ABC, Santo André, SP, Brazil*

²¹ *Universidade Federal do Rio de Janeiro, Instituto de Física, Rio de Janeiro, RJ, Brazil*

²² *Universidade Federal Fluminense, EEIMVR, Volta Redonda, RJ, Brazil*

²³ *Rudjer Bošković Institute, 10000 Zagreb, Croatia*

²⁴ *Charles University, Faculty of Mathematics and Physics, Institute of Particle and Nuclear Physics, Prague, Czech Republic*

²⁵ *Institute of Physics of the Academy of Sciences of the Czech Republic, Prague, Czech Republic*

²⁶ *Palacky University, RCPTM, Olomouc, Czech Republic*

²⁸ *Institut de Physique Nucléaire d'Orsay (IPNO), Université Paris 11, CNRS-IN2P3, Orsay, France*

France

²⁹ *Laboratoire AstroParticule et Cosmologie (APC), Université Paris 7, CNRS-IN2P3, Paris, France*

³⁰ *Laboratoire de l'Accélérateur Linéaire (LAL), Université Paris 11, CNRS-IN2P3, France*

³¹ *Laboratoire de Physique Nucléaire et de Hautes Energies (LPNHE), Universités Paris 6 et Paris 7, CNRS-IN2P3, Paris, France*

³² *Laboratoire de Physique Subatomique et de Cosmologie (LPSC), Université Joseph Fourier Grenoble, CNRS-IN2P3, Grenoble INP, France*

³³ *SUBATECH, École des Mines de Nantes, CNRS-IN2P3, Université de Nantes, France*

³⁴ *Bergische Universität Wuppertal, Wuppertal, Germany*

³⁵ *Karlsruhe Institute of Technology - Campus North - Institut für Kernphysik, Karlsruhe, Germany*

³⁶ *Karlsruhe Institute of Technology - Campus North - Institut für Prozessdatenverarbeitung und Elektronik, Karlsruhe, Germany*

³⁷ *Karlsruhe Institute of Technology - Campus South - Institut für Experimentelle Kernphysik (IEKP), Karlsruhe, Germany*

³⁸ *Max-Planck-Institut für Radioastronomie, Bonn, Germany*

³⁹ *RWTH Aachen University, III. Physikalisches Institut A, Aachen, Germany*

⁴⁰ *Universität Hamburg, Hamburg, Germany*

⁴¹ *Universität Siegen, Siegen, Germany*

⁴² *Dipartimento di Fisica dell'Università and INFN, Genova, Italy*

⁴³ *Università dell'Aquila and INFN, L'Aquila, Italy*

⁴⁴ *Università di Milano and Sezione INFN, Milan, Italy*

⁴⁵ *Università di Napoli "Federico II" and Sezione INFN, Napoli, Italy*

⁴⁶ *Università di Roma II "Tor Vergata" and Sezione INFN, Roma, Italy*

⁴⁷ *Università di Catania and Sezione INFN, Catania, Italy*

⁴⁸ *Università di Torino and Sezione INFN, Torino, Italy*

⁴⁹ *Dipartimento di Matematica e Fisica "E. De Giorgi" dell'Università del Salento and Sezione INFN, Lecce, Italy*

⁵⁰ *Istituto di Astrofisica Spaziale e Fisica Cosmica di Palermo (INAF), Palermo, Italy*

⁵¹ *Istituto di Fisica dello Spazio Interplanetario (INAF), Università di Torino and Sezione INFN, Torino, Italy*

⁵² *INFN, Laboratori Nazionali del Gran Sasso, Assergi (L'Aquila), Italy*

⁵³ *Benemérita Universidad Autónoma de Puebla, Puebla, Mexico*

⁵⁴ *Centro de Investigación y de Estudios Avanzados del IPN (CINVESTAV), México, Mexico*

⁵⁵ *Universidad Michoacana de San Nicolas de Hidalgo, Morelia, Michoacan, Mexico*

⁵⁶ *Universidad Nacional Autonoma de Mexico, Mexico, D.F., Mexico*

⁵⁷ *IMAPP, Radboud University Nijmegen, Netherlands*

⁵⁸ *Kernfysisch Versneller Instituut, University of Groningen, Groningen, Netherlands*

⁵⁹ *Nikhef, Science Park, Amsterdam, Netherlands*

- ⁶⁰ ASTRON, Dwingeloo, Netherlands
⁶¹ Institute of Nuclear Physics PAN, Krakow, Poland
⁶² University of Lódz, Lódz, Poland
⁶³ LIP and Instituto Superior Técnico, Technical University of Lisbon, Portugal
⁶⁴ 'Horia Hulubei' National Institute for Physics and Nuclear Engineering, Bucharest- Magurele, Romania
⁶⁵ University of Bucharest, Physics Department, Romania
⁶⁶ University Politehnica of Bucharest, Romania
⁶⁷ J. Stefan Institute, Ljubljana, Slovenia
⁶⁸ Laboratory for Astroparticle Physics, University of Nova Gorica, Slovenia
⁶⁹ Instituto de Física Corpuscular, CSIC-Universitat de València, Valencia, Spain
⁷⁰ Universidad Complutense de Madrid, Madrid, Spain
⁷¹ Universidad de Alcalá, Alcalá de Henares (Madrid), Spain
⁷² Universidad de Granada & C.A.F.P.E., Granada, Spain
⁷³ Universidad de Santiago de Compostela, Spain
⁷⁴ Rudolf Peierls Centre for Theoretical Physics, University of Oxford, Oxford, United Kingdom
⁷⁵ School of Physics and Astronomy, University of Leeds, United Kingdom
⁷⁶ Argonne National Laboratory, Argonne, IL, USA
⁷⁷ Case Western Reserve University, Cleveland, OH, USA
⁷⁸ Colorado School of Mines, Golden, CO, USA
⁷⁹ Colorado State University, Fort Collins, CO, USA
⁸⁰ Colorado State University, Pueblo, CO, USA
⁸¹ Fermilab, Batavia, IL, USA
⁸² Los Alamos National Laboratory, Los Alamos, NM, USA
⁸³ Louisiana State University, Baton Rouge, LA, USA
⁸⁴ Michigan Technological University, Houghton, MI, USA
⁸⁵ New York University, New York, NY, USA
⁸⁶ Northeastern University, Boston, MA, USA
⁸⁷ Ohio State University, Columbus, OH, USA
⁸⁸ Pennsylvania State University, University Park, PA, USA
⁹⁰ University of Chicago, Enrico Fermi Institute, Chicago, IL, USA
⁹¹ University of Hawaii, Honolulu, HI, USA
⁹² University of Nebraska, Lincoln, NE, USA
⁹³ University of New Mexico, Albuquerque, NM, USA
⁹⁴ University of Wisconsin, Madison, WI, USA
⁹⁵ University of Wisconsin, Milwaukee, WI, USA
⁹⁶ Institute for Nuclear Science and Technology (INST), Hanoi, Vietnam
 (†) Deceased
 (a) at Konan University, Kobe, Japan
(b) now at the Universidad Autonoma de Chiapas on leave of absence from Cinvestav

- (f) now at University of Maryland
- (h) now at NYU Abu Dhabi
- (i) now at Université de Lausanne

ABSTRACT

A thorough search for large scale anisotropies in the distribution of arrival directions of cosmic rays detected above 10^{18} eV at the Pierre Auger Observatory is reported. For the first time, these large scale anisotropy searches are performed as a function of both the right ascension and the declination and expressed in terms of dipole and quadrupole moments. Within the systematic uncertainties, no significant deviation from isotropy is revealed. Upper limits on dipole and quadrupole amplitudes are derived under the hypothesis that any cosmic ray anisotropy is dominated by such moments in this energy range. These upper limits provide constraints on the production of cosmic rays above 10^{18} eV, since they allow us to challenge an origin from stationary galactic sources densely distributed in the galactic disk and emitting predominantly light particles in all directions.

Subject headings: astroparticle physics — cosmic rays

The large scale distribution of arrival directions of Ultra-High Energy Cosmic Rays (UHECRs) as a function of the energy is a key observable to provide further understanding of their origin. Above $\simeq 0.25$ EeV, the most stringent bounds ever obtained on the dipole component in the equatorial plane were recently reported, being below 2% at 99% *C.L.* for EeV energies (Auger Collaboration 2011a). Such a sensitivity provides some constraints upon scenarios in which dipolar anisotropies could be imprinted in the distribution of arrival directions as the result of the escape of UHECRs from the Galaxy up to the ankle energy (Ptuskin *et al.* 1993; Candia *et al.* 2003; Giacinti *et al.* 2012). On the other hand, if UHECRs above 1 EeV have already a predominant extragalactic origin (Hillas 1967; Blumenthal 1970; Berezinsky *et al.* 2006; Berezinsky *et al.* 2004), their angular distribution is expected to be isotropic to a high level. Thus, the study of large scale anisotropies at EeV energies would help in establishing whether the origin of UHECRs is galactic or extragalactic in this energy range.

The upper limits aforementioned are based on first harmonic analyses of the right ascension distributions in several energy ranges. The analyses benefit from the almost uniform directional exposure in right ascension of any ground based observatory operating with high duty cycle, but are not sensitive to a dipole component along the Earth rotation axis. In contrast, using the large amount of data collected by the surface detector array of the Pierre Auger Observatory, we report in this letter on searches for dipole and quadrupole patterns significantly standing out above the background noise whose components are functions of *both* the right ascension and the declination (a detailed description of the present analysis can be found in (Auger Collaboration 2012)).

The Pierre Auger Observatory is located in Malargüe, Argentina, at mean latitude 35.2° S, mean longitude 69.5° W and mean altitude 1400 meters above sea level. It exploits two available techniques to detect extensive air showers initiated by UHECRs : a *Surface Detector (SD) array* and a *Fluorescence Detector (FD)*. The SD array consists of 1660 water-Cherenkov detectors laid out over about 3000 km^2 on a triangular grid with 1.5 km spacing, sensitive to the light emitted in their volume by the secondary particles of the showers. At the perimeter of this array, the atmosphere is overlooked on dark nights by 27 optical telescopes grouped in 5 buildings. These telescopes record the number of secondary charged particles in the air shower as a function of depth in the atmosphere by measuring the amount of nitrogen fluorescence caused by those particles along the track of the shower. At the lowest energies observed, the angular resolution of the SD is about 2.2° , and reaches $\sim 1^\circ$ at the highest energies. This is sufficient to perform searches for large-scale anisotropies. The statistical fluctuation in energy measurement amounts to about 15%, while the absolute energy scale is given by the FD measurements and has a systematic uncertainty of 22% (Auger Collaboration 2008).

In the analyses presented in this letter, the data set consists of events recorded by the SD array from 1 January 2004 to 31 December 2011, with zenith angles less than 55° . To ensure good reconstruction, an event is accepted only if all six nearest neighbours of the water-Cherenkov detector with the highest signal were operational at the time of the event (Auger Collaboration 2010a). Based on this fiducial cut, any active water-Cherenkov detector with six active neighbours defines an active *elemental cell*. In these conditions, and above the energy at which the detection efficiency saturates, 3 EeV (Auger Collaboration 2010a), the total exposure of the SD array is $23,520 \text{ km}^2 \text{ yr sr}$.

Due to the steepness of the energy spectrum, any mild bias in the estimate of the shower energy with time or zenith angle can lead to significant distortions of the event counting rate above a given energy. It is thus critical to control the energy estimate in searching for anisotropies. The procedure followed to obtain an unbiased estimate of the shower energy consists in correcting measurements of shower signals for the influences of weather effects (Auger Collaboration 2009) and the geomagnetic field (Auger Collaboration 2011b). Using the constant intensity cut method (Hersil 1961), the shower signal is then converted to the value that would have been expected had the shower arrived at a zenith angle 38° . This reference shower signal is finally converted into energy using a calibration curve based on hybrid events measured simultaneously by the SD array and FD telescopes, since the latter can provide a calorimetric measurement of the energy (Auger Collaboration 2008).

In searching for anisotropies, it is also critical to know accurately the effective time-integrated collecting area for a flux from each direction of the sky, or in other words, the *directional exposure* ω of the Observatory. For each elemental cell, this is obtained through the integration over Local Sidereal Time (LST) α^0 of $x^{(i)}(\alpha^0) \times a_{\text{cell}}(\theta) \times \epsilon(\theta, \varphi, E)$, with $x^{(i)}(\alpha^0)$ the total operational time of the cell (i) at LST α^0 , $a_{\text{cell}}(\theta) = 1.95 \cos \theta \text{ km}^2$ the geometric aperture of each elemental cell under incidence zenith angle θ (Auger Collaboration 2010a), and $\epsilon(\theta, \varphi, E)$ the detection efficiency under incidence zenith angle θ and azimuth angle φ at energy E . In the same way as

in (Auger Collaboration 2011a), the small modulation of the exposure in α^0 due to the variations of $x^{(i)}$ can be accounted for by re-weighting the events with the number of elemental cells at the LST of each event k , $\Delta N_{\text{cell}}(\alpha_k^0)$. Since both θ and φ depend only on the difference $\alpha - \alpha^0$, the integration over α^0 can then be substituted for an integration over the hour angle $\alpha' = \alpha - \alpha^0$ so that the directional exposure actually does not depend on right ascension when the $x^{(i)}$ are assumed to be independent of the LST :

$$\omega(\delta, E) = \sum_{i=1}^{n_{\text{cell}}} x^{(i)} \int_0^{24h} d\alpha' a_{\text{cell}}(\theta(\alpha', \delta)) \epsilon(\theta(\alpha', \delta), \varphi(\alpha', \delta), E). \quad (1)$$

The zenithal dependence of the detection efficiency $\epsilon(\theta, \varphi, E)$ can be obtained directly from the data in an empirical way (Auger Collaboration 2012). Additional effects have an impact on ω , such as the azimuthal dependence of the efficiency due to geomagnetic effects, the corrections to both the geometric aperture of each elemental cell and the detection efficiency due to the tilt of the array, and the corrections due to the spatial extension of the array. Accounting for all these effects, the resulting dependence of ω on declination can be found in (Auger Collaboration 2012). For a wide range of declinations between $\simeq -89^\circ$ and $\simeq -20^\circ$, the directional exposure is $\simeq 2,500 \text{ km}^2 \text{ yr}$ at 1 EeV, and $\simeq 3,500 \text{ km}^2 \text{ yr}$ for any energy above full efficiency. Then, at higher declinations, it smoothly falls to zero, with no exposure above 20° declination.

The detection of significant dipole or quadrupole moments above EeV energies would be of considerable interest. Dipole and quadrupole patterns are encoded in the low order a_{1m} and a_{2m} coefficients of the multipolar expansion of any angular distribution over the sphere $\Phi(\mathbf{n})$:

$$\Phi(\mathbf{n}) = \sum_{\ell \geq 0} \sum_{m=-\ell}^{\ell} a_{\ell m} Y_{\ell m}(\mathbf{n}), \quad (2)$$

where \mathbf{n} denotes a unit vector taken in equatorial coordinates. Due to the non-uniform and incomplete coverage of the sky at the Pierre Auger Observatory, the estimated coefficients $\bar{a}_{\ell m}$ are determined in a two-step procedure. First, from any event set with arrival directions $\{\mathbf{n}_1, \dots, \mathbf{n}_N\}$ recorded at LST $\{\alpha_1^0, \dots, \alpha_N^0\}$, the multipolar coefficients of the angular distribution coupled to the exposure function are estimated through :

$$\bar{b}_{\ell m} = \sum_{k=1}^N \frac{Y_{\ell m}(\mathbf{n}_k)}{\Delta N_{\text{cell}}(\alpha_k^0)}. \quad (3)$$

$\Delta N_{\text{cell}}(\alpha_k^0)$ corrects for the slightly non-uniform directional exposure in right ascension. Then, assuming that the multipolar expansion of the angular distribution $\Phi(\mathbf{n})$ is *bounded* to ℓ_{\max} , the first $b_{\ell m}$ coefficients with $\ell \leq \ell_{\max}$ are related to the non-vanishing $a_{\ell m}$ through :

$$\bar{b}_{\ell m} = \sum_{\ell'=0}^{\ell_{\max}} \sum_{m'=-\ell'}^{\ell'} [K]_{\ell m}^{\ell' m'} \bar{a}_{\ell' m'}, \quad (4)$$

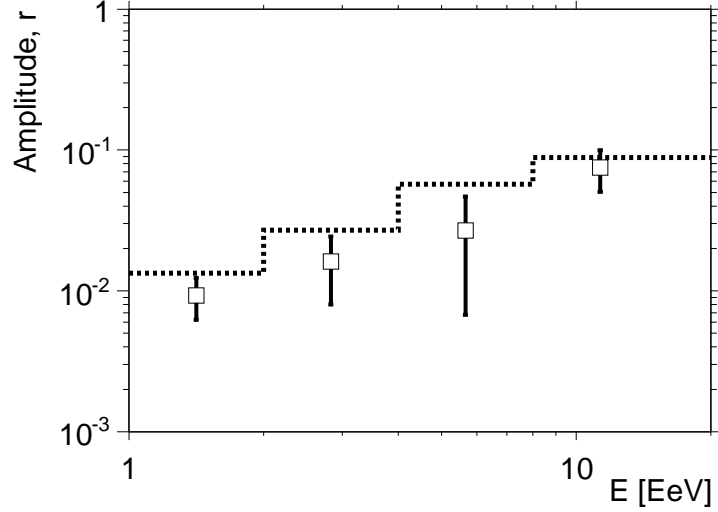


Fig. 1.— Reconstructed amplitude of the dipole as a function of the energy. The dotted line stands for the 99% *C.L.* upper bounds on the amplitudes that would result from fluctuations of an isotropic distribution.

where the matrix K is entirely determined by the directional exposure :

$$[K]_{\ell m}^{\ell' m'} = \int_{\Delta\Omega} d\Omega \omega(\mathbf{n}) Y_{\ell m}(\mathbf{n}) Y_{\ell' m'}(\mathbf{n}). \quad (5)$$

Inverting Eqn. 4 allows us to recover the underlying $\bar{a}_{\ell m}$, with a resolution proportional to $([K^{-1}]_{\ell m}^{\ell m} \bar{a}_{00})^{0.5}$ (Billoir & Deligny 2008). As a consequence of the incomplete coverage of the sky, this resolution deteriorates by a factor larger than 2 each time ℓ_{\max} is incremented by 1. With our present statistics, this prevents the recovery of each coefficient with good accuracy as soon as $\ell_{\max} \geq 3$, which is why we restrict ourselves to dipole and quadrupole searches.

We first assume that the angular distribution of cosmic rays is modulated by a *pure* dipole and parameterise the intensity $\Phi(\mathbf{n})$ in any direction as :

$$\Phi(\mathbf{n}) = \frac{\Phi_0}{4\pi} \left(1 + r \mathbf{d} \cdot \mathbf{n} \right), \quad (6)$$

where \mathbf{d} denotes the dipole unit vector. The dipole pattern is here fully characterised by a declination δ_d , a right ascension α_d , and an amplitude r corresponding to the maximal anisotropy contrast : $r = (\Phi_{\max} - \Phi_{\min}) / (\Phi_{\max} + \Phi_{\min})$. The estimation of these three coefficients is straightforward from the estimated spherical harmonic coefficients \bar{a}_{1m} . The reconstructed amplitudes \bar{r} are shown in Fig. 1 as a function of the energy. The 99% *C.L.* upper bounds on the amplitudes that would result from fluctuations of an isotropic distribution are indicated by the dotted line. One can see that within the statistical uncertainties, there is no evidence of any significant signal. In Fig. 2, the corresponding directions are shown in orthographic projection with the associated uncertainties, as a function of the energy. Both angles are expected to be randomly distributed

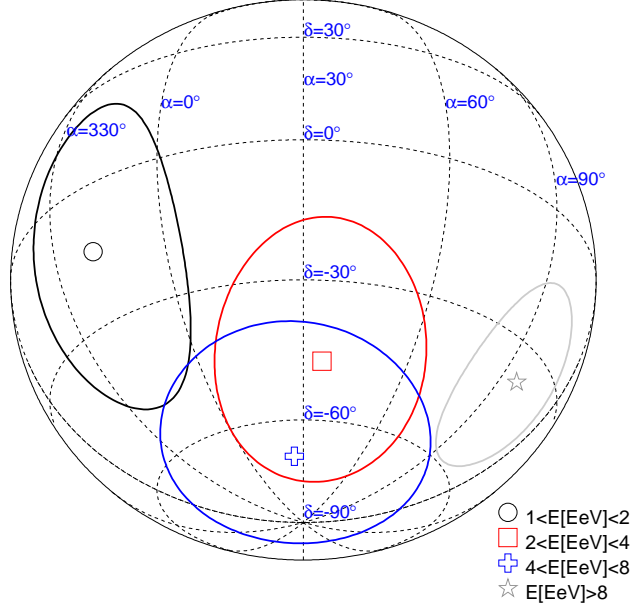


Fig. 2.— Reconstructed declination and right-ascension of the dipole with corresponding uncertainties, as a function of the energy, in orthographic projection.

in the case of independent samples whose parent distribution is isotropic. It is thus interesting to note that all reconstructed declinations are in the equatorial southern hemisphere, and to note also the intriguing smooth alignment of the phases in right ascension as a function of the energy. In our previous report on first harmonic analysis in right ascension (Auger Collaboration 2011a), we already pointed out this alignment, and stressed that such a consistency of phases in adjacent energy intervals is expected with smaller number of events than the detection of amplitudes standing-out significantly above the background noise in the case of a real underlying anisotropy. This motivated us to design a *prescription* aimed at establishing at 99% *C.L.* whether this consistency in phases is real, using the exact same analysis as the one reported in (Auger Collaboration 2011a). The prescribed test will end once the total exposure since 25 June 2011 reaches 21,000 km² yr sr. The smooth fit to the data of (Auger Collaboration 2011a) is shown as a dashed line in Fig 3, restricted to the energy range considered here. Though the phase between 4 and 8 EeV is poorly determined due to the corresponding direction in declination pointing close to the equatorial south pole, it is noteworthy that a consistent smooth behaviour is observed using the analysis presented here and applied to a data set containing two additional years of data.

Assuming now that the angular distribution of cosmic rays is modulated by a dipole *and* a quadrupole, the intensity $\Phi(\mathbf{n})$ can be parameterised in any direction \mathbf{n} as :

$$\Phi(\mathbf{n}) = \frac{\Phi_0}{4\pi} \left(1 + r \mathbf{d} \cdot \mathbf{n} + \lambda_+ (\mathbf{q}_+ \cdot \mathbf{n})^2 + \lambda_0 (\mathbf{q}_0 \cdot \mathbf{n})^2 + \lambda_- (\mathbf{q}_- \cdot \mathbf{n})^2 \right), \quad (7)$$

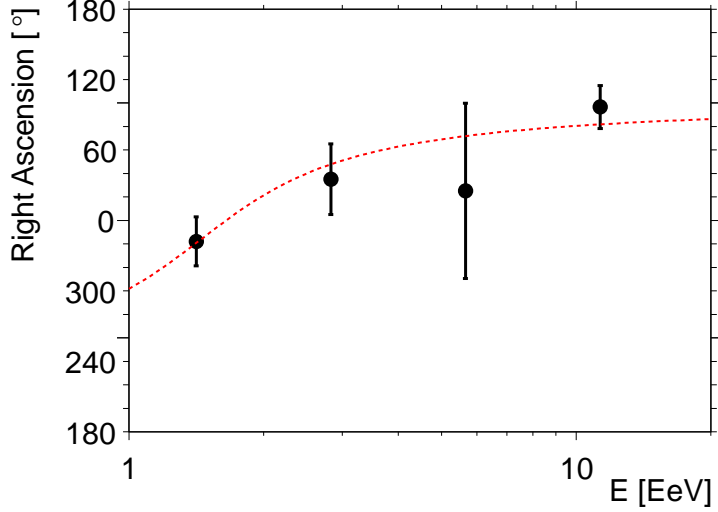


Fig. 3.— Reconstructed right ascension of the dipole as a function of the energy. The smooth fit to the data of (Auger Collaboration 2011a) is shown as the dashed line (see text).

with the constraint $\lambda_+ + \lambda_- + \lambda_0 = 0$. It is convenient to define the quadrupole amplitude $\beta \equiv (\lambda_+ - \lambda_-)/(2 + \lambda_+ + \lambda_-)$, which provides a measure of the maximal quadrupolar contrast in the absence of a dipole. Hence, any quadrupolar pattern can be fully described by two amplitudes (β, λ_+) and three angles : (δ_+, α_+) which define the orientation of \mathbf{q}_+ and (α_-) which defines the direction of \mathbf{q}_- in the orthogonal plane to \mathbf{q}_+ . The third eigenvector \mathbf{q}_0 is orthogonal to \mathbf{q}_+ and \mathbf{q}_- . The estimated amplitudes $\bar{\lambda}_+$ and $\bar{\beta}$ are shown in Fig. 4 as functions of the energy. In the same way as for dipole amplitudes, the 99% *C.L.* upper bounds on the quadrupole amplitude that could result from fluctuations of an isotropic distribution are indicated by the dashed lines. Throughout the energy range, there is no evidence for anisotropy.

There are small uncertainties in correcting the estimator of the energy for weather and geomagnetic effects, and these propagate into systematic uncertainties in the measured anisotropy parameters. As well, anisotropy parameters may be altered in a systematic way by energy dependence of the attenuation curve. All these systematic effects have been quantified (Auger Collaboration 2012). They do not change significantly the results presented here.

From these analyses, upper limits on dipole and quadrupole amplitudes can be derived at 99% *C.L.*. They are shown in Fig. 5 for the dipole amplitudes, accounting for the systematic uncertainties. We illustrate now their astrophysical interest by calculating the amplitudes of anisotropy expected in a toy scenario in which sources of EeV-cosmic rays are stationary, densely and uniformly distributed in the galactic disk, and emit particles in all directions.

Both the strength and the structure of the magnetic field in the Galaxy, known only approximately, play a crucial role in the propagation of cosmic rays. The field is thought to contain a large scale regular component and a small scale turbulent one, both having a local strength of a

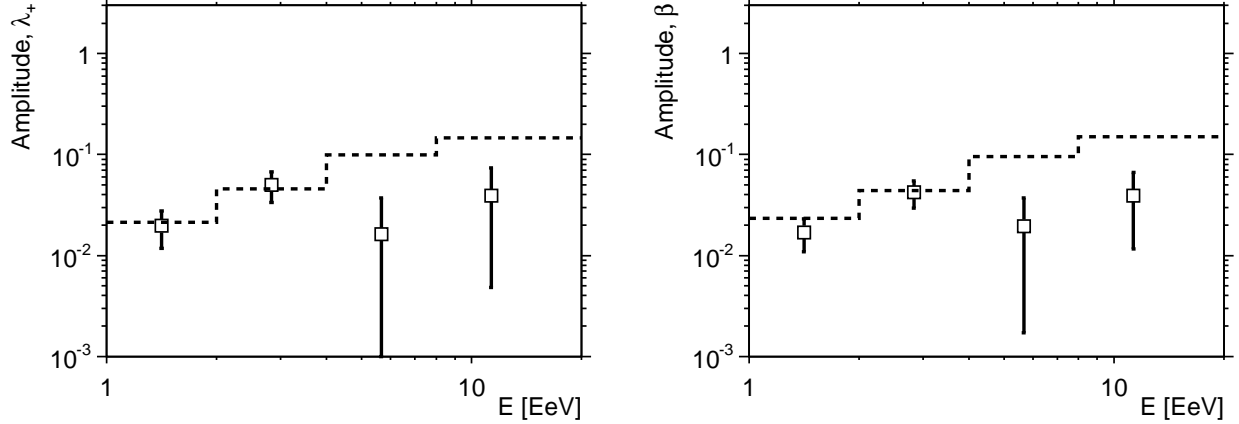


Fig. 4.— Amplitudes of the quadrupolar moment as a function of the energy using a multipolar reconstruction up to $\ell_{\max} = 2$. The dotted lines stand for the 99% *C.L.* upper bounds on the amplitudes that could result from fluctuations of an isotropic distribution.

few microgauss (see *e.g.* (Beck 2001)). While the turbulent component dominates in strength by a factor of a few, the regular component imprints dominant drift motions as soon as the Larmor radius of cosmic rays is larger than the maximal scale of the turbulences (thought to be in the range 10-100 pc). We adopt here a recent parameterisation of the regular component obtained by fitting model field geometries to Faraday rotation measures of extragalactic radio sources and polarised synchrotron emission (BSS-model, with anti-symmetric halo with respect to the galactic plane) (Pshirkov *et al.* 2011). In addition to the regular component, a turbulent field is generated according to a Kolmogorov power spectrum and is pre-computed on a three dimensional grid periodically repeated in space. The size of the grid is selected to match the maximal scale of turbulences (taken here as 100 pc), and the strength of the turbulent component is taken as three times the strength of the regular one. To describe the propagation of cosmic rays with energies $E \geq 1$ EeV in such a magnetic field, the direct integration of trajectories is the most appropriate tool. To obtain the anisotropy of cosmic rays emitted from sources uniformly distributed in a cylinder with a radius of 20 kpc from the galactic centre and with a height of ± 100 pc, we adopt a method first proposed in (Thielheim & Langhoff 1968). It consists in back-tracking anti-particles with random directions from the Earth to outside the Galaxy. Each test particle *probes* the total luminosity along the path of propagation from each direction as seen from the Earth. For *stationary sources emitting cosmic rays in all directions*, the expected flux in the initial sampled direction is proportional to the time spent by each test particle in the source region.

The amplitudes of anisotropy obviously depend on the rigidity E/Z of the cosmic rays, with Z the electric charge of the particles. Since we only aim at illustrating the upper limits, we consider two extreme single primaries : protons and iron nuclei. The calculation of anisotropy amplitudes for single primaries is useful to probe the allowed contribution of each primary as a function of the energy.

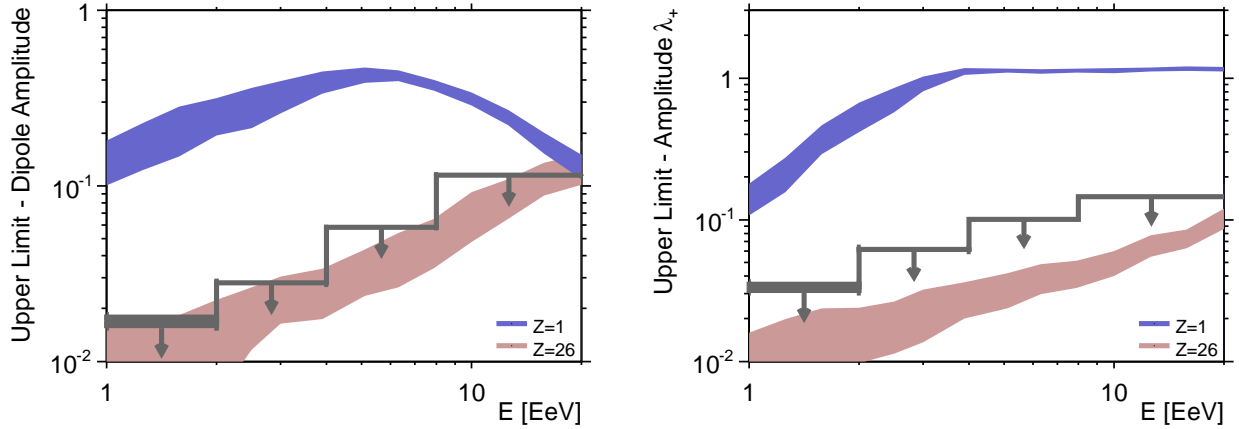


Fig. 5.— 99% *C.L.* upper limits on dipole and quadrupole amplitudes as a function of the energy. Some generic anisotropy expectations from stationary galactic sources distributed in the disk are also shown, for various assumptions on the cosmic ray composition. The fluctuations of the amplitudes due to the stochastic nature of the turbulent component of the magnetic field are sampled from different simulation data sets and are shown by the bands.

The dipole and quadrupole amplitudes obtained for several energy values covering the range $1 \leq E/\text{EeV} \leq 20$ are shown in Fig. 5. To probe unambiguously amplitudes down to the percent level, it is necessary to generate simulated event sets with at least $\simeq 5 \cdot 10^5$ test particles. Such a number of simulated events allows us to shrink statistical uncertainties on amplitudes at the 0.5% level. Meanwhile, there is an intrinsic variance in the model for each anisotropy parameter due to the stochastic nature of the turbulent component of the magnetic field. This variance is estimated through the simulation of 20 sets of $5 \cdot 10^5$ test particles, where the configuration of the turbulent component is frozen in each set. The RMS of the amplitudes sampled in this way is shown by the bands in Fig. 5.

The resulting amplitudes for protons largely stand above the allowed limits. Consequently, unless the strength of the magnetic field is much higher than in the picture used here, the upper limits derived in this analysis exclude that the light component of cosmic rays comes from galactic stationary sources densely distributed in the galactic disk and emitting in all directions. To respect the dipole limits below the ankle energy, the fraction of protons should not exceed $\simeq 10\%$ of the cosmic ray composition. This is particularly interesting in the view of the indications for the presence of a light component around 1 EeV from shower depth maximum measurements (Auger Collaboration 2010b; Abbasi *et al.* 2010; Jui *et al.* 2011), though firm interpretations of these measurements in terms of the atomic mass still suffer from some ambiguity due to the uncertain hadronic interaction models used to describe the shower developments. On the other hand, if the cosmic ray composition around 1 EeV results from a mixture containing heavy elements of galactic origin and light elements of extragalactic origin, upper limits can be respected. This is because large scale anisotropy amplitudes below the percent level are expected for extragalactic

cosmic rays, due to the motion of the Galaxy relative to a possibly stationary extragalactic cosmic ray rest frame (Kachelriess & Serpico 2006; Harari *et al.* 2010).

Future measurements of composition below 1 EeV will come from the low energy extension HEAT now available at the Pierre Auger Observatory (Mathes *et al.* 2011). Combining these measurements with large scale anisotropy ones will then allow us to further understand the origin of cosmic rays at energies less than 4 EeV.

Acknowledgements

The successful installation, commissioning, and operation of the Pierre Auger Observatory would not have been possible without the strong commitment and effort from the technical and administrative staff in Malargüe.

We are very grateful to the following agencies and organizations for financial support: Comisión Nacional de Energía Atómica, Fundación Antorchas, Gobierno De La Provincia de Mendoza, Municipalidad de Malargüe, NDM Holdings and Valle Las Leñas, in gratitude for their continuing cooperation over land access, Argentina; the Australian Research Council; Conselho Nacional de Desenvolvimento Científico e Tecnológico (CNPq), Financiadora de Estudos e Projetos (FINEP), Fundação de Amparo à Pesquisa do Estado de Rio de Janeiro (FAPERJ), Fundação de Amparo à Pesquisa do Estado de São Paulo (FAPESP), Ministério de Ciência e Tecnologia (MCT), Brazil; AVCR AV0Z10100502 and AV0Z10100522, GAAV KJB100100904, MSMT-CR LA08016, LG11044, MEB111003, MSM0021620859, LA08015 and TACR TA01010517, Czech Republic; Centre de Calcul IN2P3/CNRS, Centre National de la Recherche Scientifique (CNRS), Conseil Régional Ile-de-France, Département Physique Nucléaire et Corpusculaire (PNC-IN2P3/CNRS), Département Sciences de l'Univers (SDU-INSU/CNRS), France; Bundesministerium für Bildung und Forschung (BMBF), Deutsche Forschungsgemeinschaft (DFG), Finanzministerium Baden-Württemberg, Helmholtz-Gemeinschaft Deutscher Forschungszentren (HGF), Ministerium für Wissenschaft und Forschung, Nordrhein-Westfalen, Ministerium für Wissenschaft, Forschung und Kunst, Baden-Württemberg, Germany; Istituto Nazionale di Fisica Nucleare (INFN), Ministero dell'Istruzione, dell'Università e della Ricerca (MIUR), Italy; Consejo Nacional de Ciencia y Tecnología (CONACYT), Mexico; Ministerie van Onderwijs, Cultuur en Wetenschap, Nederlandse Organisatie voor Wetenschappelijk Onderzoek (NWO), Stichting voor Fundamenteel Onderzoek der Materie (FOM), Netherlands; Ministry of Science and Higher Education, Grant Nos. N N202 200239 and N N202 207238, Poland; Portuguese national funds and FEDER funds within COMPETE - Programa Operacional Factores de Competitividade through Fundação para a Ciência e a Tecnologia, Portugal; Romanian Authority for Scientific Research, UEFICDI, Ctr.Nr.1/ASPERA2 ERA-NET, Romania; Ministry for Higher Education, Science, and Technology, Slovenian Research Agency, Slovenia; Comunidad de Madrid, FEDER funds, Ministerio de Ciencia e Innovación and Consolider-Ingenio 2010 (CPAN), Xunta de Galicia, Spain; Science and Technology Facilities Council, United Kingdom; Department of Energy, Contract Nos. DE-AC02-07CH11359, DE-FR02-04ER41300, National Science

Foundation, Grant No. 0450696, The Grainger Foundation USA; NAFOSTED, Vietnam; Marie Curie-IRSES/EPLANET, European Particle Physics Latin American Network, European Union 7th Framework Program, Grant No. PIRSES-2009-GA-246806; and UNESCO.

REFERENCES

- Abbasi, R. U. *et al.* (The HiRes Collaboration) 2010, Phys. Rev. Lett. 104 161101
- Beck, R. 2001, Space Sci. Rev. 99 243
- Berezinsky, V. S., Grigorieva, S. I. & Hnatyk, B. I. 2004, Astropart. Phys. 21 617625
- Berezinsky, V. S., Gazizov, A. Z., & Grigorieva, S. I. 2006, Phys. Rev. D 74 043005
- Billoir, P. & Deligny, O. 2008, JCAP 02 009
- Blumenthal, G. R. 1970, Phys. Rev. D1 1596
- Bonifazi, C., for the Pierre Auger Collaboration 2009, Nucl. Phys. Proc. Suppl. 190 20
- Candia, J., Mollerach, S. & Roulet, E. 2003, JCAP 0305 003
- Giacinti, G. *et al.* 2012, JCAP 07 031
- Harari, D., Mollerach, S. & Roulet, E. 2010, JCAP 11 033
- Hersil, J. *et al.* 1961, Phys. Rev. Lett. 6 22
- Hillas, A. M. 1967, Phys. Lett. 24A 677
- Jui, C. C. H. *et al.* (The Telescope Array Collaboration) 2011, Proceedings of the APS meeting, arXiv:1110.0133
- Kachelriess, M. & Serpico, P. 2006, Phys. Lett. B 640 225-229
- Mathes, H. J., for the Pierre Auger Collaboration 2011, Proceedings of the 32nd ICRC, Beijing
- The Pierre Auger Collaboration 2008, Phys. Rev. Lett. 101 061101
- The Pierre Auger Collaboration 2009, Astropart. Phys. 32 89
- The Pierre Auger Collaboration 2010a, Nucl. Instr. and Meth. A 613 29
- The Pierre Auger Collaboration 2010b, Phys. Rev. Lett. 104 091101
- The Pierre Auger Collaboration 2011a, Astropart. Phys. 34 627-639
- The Pierre Auger Collaboration 2011b, JCAP 11 022

The Pierre Auger Collaboration 2012, ApJS 203 34

Pshirkov, M. S. *et al.* 2011, ApJ 738 192

Ptuskin, V. *et al.* 1993, Astron. Astrophys. 268 726

Sanchez, F., for the Pierre Auger Collaboration 2011, Proceedings of the 32nd ICRC, Beijing

Thielheim, K. O. & Langhoff, W. 1968, J. Phys. A 694

Zirakashvili, V. N. *et al.* 1998, AstL. 24 139